Volume III N° 11 V3N11A2021
Revue de l'Entrepreneuriat et de l'Innovation

Electrical energy harvesting from a nonlinear oscillator using a delayed piezoelectric circuit

Zakaria Ghouli

Polydisciplinary Faculty of Taroudant, University Ibn Zohr, Taroudant, Morocco

ghoulizakaria@gmail.com
z.ghouli@uiz.ac.ma

Résumé- ***We investigate quasi-periodic (QP) vibration-based energy harvesting (EH) in a harmonically excited van der Pol oscillator coupled to a delayed piezoelectric coupling mechanism. The case of primary resonance, for which the frequency of the harmonic excitation is near the natural frequency of the oscillator, is considered. Analytical approximation of the QP response and the corresponding power output are obtained using the double-step multiple scales method. The effect of the time delay on the EH performance is studied. It is shown that for appropriate combination of time delay parameters, QP vibration can be used to scavenge energy over a broadband of the excitation frequency away from the resonance with a better performance.***

Mots-clés: Energy harvesting, van der Pol oscillator, quasi-periodic vibrations, delayed piezoelectric coupling.

I. INTRODUCTION

Quasi-periodic (QP) vibration-based energy harvesting (EH) using time delay has been widely studied in the literature [1, 2, 4-8]. The time delay has used in a Duffing-type monostable harvester device subject to a harmonic excitation and coupled to a piezoelectric circuit [1, 2]. The induced large-amplitude QP vibrations have been exploited to enhance EH performance. It was shown that for appropriate values of delay parameters, QP vibration-based EH can be exploited to extract energy over a broadband of excitation frequencies away from the resonance with good efficiency, thereby avoiding hysteresis and bistability near the resonance. In [1, 2] the time delay is introduced in the mechanical subsystem. The case where the time delay is introduced in the electrical circuit was studied in [3]. It is shown that for appropriate values of delay amplitude, the energy harvesting performance is improved over a certain range of coupling parameters and excitation frequencies.

In [4], it was reported that in a delayed van der Pol oscillator with modulated delay amplitude coupled to an electromagnetic energy harvester, large-amplitude QP vibrations performing in broad range of parameters could be exploited to scavenge energy. In [4] the time delay is introduced in the mechanical subsystem. The case where the time delay is introduced in both mechanical component and electrical circuit was studied in [5]. It is shown that for appropriate values of amplitudes and frequency of time delay the maximum output power of the harvester is not necessarily accompanied by the maximum amplitude of system response. Recently, QP vibration-based EH in a delayed nonlinear MEMS device consisting of a delayed Mathieu-van der Pol-Duffing type oscillator coupled to a delayed piezoelectric coupling mechanism was investigated in [6]. It was shown that QP vibrations could be exploited to extract energy with good performance compared to periodic vibrations.

In [7] we present a review on the recent results on QP vibration-based EH in a van der Pol oscillator with time-periodic delay amplitude coupled either

to undelayed electromagnetic component or to delayed electromagnetic one. More recently, it was reported that in a delayed Duffing oscillator, the modulation of the delay amplitude near the delay parametric resonance gives rise to large-amplitude QP vibration which is exploited to extract energy with better performance comparing to the periodic output power [8].

Taking advantage from using QP vibrations to extract energy from EH system in the case of the time delay is included within the piezoelectric coupling as a controller [3, 5, 6], the purpose of the present work is to study the EH performance in the case of a van der Pol-type harvester device subject to a harmonic excitation and coupled to an electric circuit through a delayed piezoelectric coupling mechanism. Here we explore the effect of a time delayed introduced in the piezoelectric subsystem on the EH performance of the system. Moreover, introduction of time delay in the piezoelectric coupling can be viewed as a technique for controlling and optimizing the output power of the harvester.

The rest of the paper is structured as follows. Section 2 describes the harvester system and gives an approximation of the periodic response and the amplitude of the harvested power near the primary resonance using the multiple scales method. In Section 3, the QP response is approximated applying the second-step multiple scales method and the corresponding harvested power is provided. The influence of time delay introduced in the electrical circuit of the harvester device on the EH performance is analyzed in Section 3 and a summary of the results is given in the concluding section.

II. Model description and periodic energy harvesting

The energy harvester device consists in van der Pol resonator coupled to electrical circuit through a piezoelectric device as shown in the schematic presented in Fig. 1. We assume that the electrical component of the harvester is under a time delayed feedback such that the governing equation for the system can be written in the dimensionless form as

$$\ddot{x}(t) + x(t) - [\alpha - \beta x(t)^2]\dot{x}(t) - \chi v(t) = f\cos(\omega t) \quad (1)$$

$$\dot{v}(t) + \mu v(t) + \kappa \dot{x}(t) = \lambda v(t-\tau) \quad (2)$$

where $x(t)$ is the relative displacement of the rigid mass m, f, ω are, respectively, the amplitude and the frequency of the harmonic excitation, $v(t)$ is the voltage across the load resistance, α and β are the mechanical damping ratio, χ is the piezoelectric coupling term in the mechanical attachment, κ is the piezoelectric coupling term in the electrical circuit, μ is the reciprocal of the time constant of the electrical circuit, λ and τ, are respectively, the feedback gain and the time delay in the electric circuit.

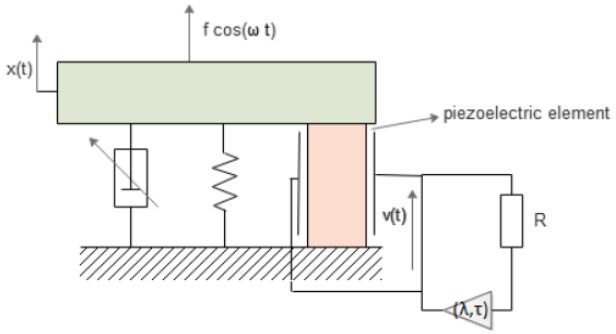

Figure 1: Schematic description of the energy harvesting system

We investigate the response of the system near the principal resonance by introducing the resonance condition $1 = \omega^2 + \sigma$ where σ is a detuning parameter. The method of multiple scales [9] is implemented by introducing a bookkeeping parameter ϵ such that parameters can be scaled as

$\alpha = \epsilon\tilde{\alpha}, \beta = \epsilon\tilde{\beta}, \chi = \epsilon\tilde{\chi}, f = \epsilon\tilde{f}, \sigma = \epsilon\tilde{\sigma}$. Thus, Eqs. (1) and (2) take the form

$$\ddot{x}(t) + \omega^2 x(t) = \epsilon[(\tilde{\alpha} - \tilde{\beta}x(t)^2)\dot{x}(t) + \tilde{\chi}v(t) + \tilde{f}\cos(\omega t) - \tilde{\sigma}x(t)] \quad (3)$$

$$\dot{v}(t) + \mu v(t) + \kappa\dot{x}(t) = \lambda v(t-\tau) \quad (4)$$

A solution to Eqs. (3) and (4) can be sought in the forme

$$x(t) = x_0(T_0, T_1) + \epsilon x_1(T_0, T_1) + O(\epsilon^2) \quad (5)$$

$$v(t) = v_0(T_0, T_1) + \epsilon v_1(T_0, T_1) + O(\epsilon^2) \quad (6)$$

Where $T_0 = t$, and $T_1 = \epsilon t$. In terms of the variables T_i, the time derivatives become $\frac{d}{dt} = D_0 + \epsilon D_1 + O(\epsilon^2)$ and $\frac{d^2}{dt^2} = D_0^2 + \epsilon^2 D_1^2 + 2\epsilon D_0 D_1 + O(\epsilon^2)$ where $D_i^j = \frac{\partial^j}{\partial^j T_i}$. Substituting (5) and (6) into (3) and (4) and equating coefficient of like powers of ϵ, we obtain up to the second order the following hierarchy of problems:

$$D_0^2 x_0 + \omega^2 x_0 = 0 \quad (7)$$

$$D_0 v_0 + \mu v_0 + \kappa D_0 x_0 = \lambda v_{0\tau} \quad (8)$$

$$D_0^2 x_1 + \omega^2 x_1 = -2D_0 D_1 x_0 + (\tilde{\alpha} - \tilde{\beta}x_0^2)D_0 x_0 - \tilde{\sigma}x_0 + \tilde{\chi}v_0 + \tilde{f}\cos(\omega t) \quad (9)$$

$$D_0 v_1 + \mu v_1 = -D_1 v_0 - \kappa D_0 x_1 - \kappa D_1 x_0 + \lambda v_{1\tau} \quad (10)$$

Up to the first order the solution is given by

$$x_0(T_0, T_1) = A(T_1)e^{i\omega T_0} + \bar{A}(T_1)e^{-i\omega T_0} \quad (11)$$

$$v_0(T_0, T_1) = \frac{-\kappa i\omega A(T_1)}{\mu + i\omega - \lambda e^{-i\omega\tau}} e^{i\omega T_0} + \frac{\kappa i\omega \bar{A}(T_1)}{\mu - i\omega - \lambda e^{i\omega\tau}} e^{-i\omega T_0} \quad (12)$$

Where $A(T_1)$ and $\bar{A}(T_1)$ are unknown complex conjugate functions. Substituting equations (11) and (12) into (9) and (10) and eliminating the secular terms, one obtains:

$$-2i\omega(D_1 A) + i\tilde{\alpha}\omega A - i\tilde{\beta}\omega A^2\bar{A} - \tilde{\sigma}A - \frac{\kappa i\omega\tilde{\chi}A}{\mu + i\omega - \lambda e^{-i\omega\tau}} + \frac{\tilde{f}}{2} = 0 \quad (13)$$

Expressing $A = \frac{1}{2}ae^{i\theta}$ where a and θ are the amplitude and the phase, we obtain up to the first order the modulation equations

$$\begin{cases} \frac{da}{dt} = S_1 a + S_2 a^3 + S_3 \sin(\theta) \\ a\frac{d\theta}{dt} = S_4 a + S_3 \cos(\theta) \end{cases} \quad (14)$$

Where $S_i (i = 1, \ldots, 4)$ are given in Appendix. The solution up to the first order given by (11) and (12) can be expressed as

$$\begin{cases} x_0(T_0, T_1) = a\cos(\omega t + \theta) \\ v_0(T_0, T_1) = V\cos(\omega t + \theta + \arctan\frac{\mu - \lambda\cos(\omega\tau)}{\omega + \lambda\sin(\omega\tau)}) \end{cases} \quad (15)$$

Such that the condition $\omega + \lambda\sin(\omega\tau) \neq 0$ excluding the locations where the amplitude of the response goes to infinity must be satisfied. Moreover, the voltage amplitude V is given by

$$V = \frac{\kappa\omega}{\sqrt{(\mu - \lambda\cos(\omega\tau))^2 + (\omega + \lambda\sin(\omega\tau))^2}} a \quad (16)$$

The steady-state response of system (14), corresponding to periodic solutions of Eqs. (3) and (4), are determined by setting $\frac{da}{dt} = \frac{d\theta}{dt} = 0$. Eliminating the phase, we obtain the following four-order algebraic equation in a

$$S_2^2 a^6 + 2S_1 S_2 a^4 + (S_1^2 + S_4^2)a^2 - S_3^2 = 0 \quad (17)$$

An expression for the average power is obtained by integrating the dimensionless form of the instantaneous power $P(t) = \mu v(t)^2$ over a period T. This is given by

$$P_{av} = \frac{1}{T}\int_0^T \mu v^2 dt \quad (18)$$

Where $T = \frac{4\pi}{\omega}$. Then, the average power expressed by $P_{av} = \frac{\mu V^2}{2}$ reads

$$P_{av} = \frac{1}{2}\left(\frac{\mu\kappa^2\omega^2}{(\mu-\lambda\cos(\omega\tau))^2+(\omega+\lambda\sin(\omega\tau))^2}\right)a^2 \quad (19)$$

Where the amplitude a is obtained from Eq. (17). Using the maximization procedure, one obtains the maximum power response as

$$P_{max} = \left(\frac{\mu\kappa^2\omega^2}{(\mu-\lambda\cos(\omega\tau))^2+(\omega+\lambda\sin(\omega\tau))^2}\right)a^2 \quad (20)$$

Equations (17) and (20) are used to examine the influence of different system parameters on the steady-state response and on the maximum output power of the harvester.

III. Quasi-periodic energy harvesting

In order to approximate the QP response we apply the second-step perturbation method [10]. To this end, it is convenient to transform the polar form (14) to the following Cartesian system using the variable change $u = a\cos\theta$ and $w = -a\sin\theta$

$$\begin{cases} \frac{du}{dt} = S_4 w + \epsilon\{S_1 u + S_2 u(u^2+w^2)\} \\ \frac{dw}{dt} = -S_4 u - S_3 + \epsilon\{S_1 w + S_2 w(u^2+w^2)\} \end{cases} \quad (21)$$

Where ϵ is a new bookkeeping parameter introduced to perform the second-step perturbation analysis. A periodic solution of the slow flow (21) corresponding to the QP response of the original system (3), (4) can be expressed in the forme

$$u(t) = u_0(T_0, T_1) + \epsilon u_1(T_0, T_1) + O(\epsilon^2) \quad (22)$$

$$w(t) = w_0(T_0, T_1) + \epsilon w_1(T_0, T_1) + O(\epsilon^2) \quad (23)$$

Where $T_0 = t$ and $T_1 = \epsilon t$. In terms of the variables T_i, the time derivatives become $\frac{d}{dt} = D_0 + \epsilon D_1 + O(\epsilon^2)$ where $D_i^j = \frac{\partial^j}{\partial^j T_i}$. Substituting (22) and (23) into (21), and equating coefficient of like powers of ϵ, we obtain the following systems

$$D_0^2 u_0 + S_4^2 u_0 = -S_3 S_4 \quad (24)$$

$$S_4 w_0 = D_0 u_0 \quad (25)$$

$$D_0^2 u_1 + S_4^2 u_1 = -D_0 D_1 u_0 + S_1 D_0 u_0 + S_2 D_0 u_0 (u_0^2 + w_0^2) - S_4 D_1 w_0 + S_2 u_0 D_0 (u_0^2 + w_0^2) + S_4 S_1 w_0 + S_4 S_2 w_0 (u_0^2 + w_0^2) \quad (26)$$

$$S_4 w_1 = D_0 u_1 + D_1 u_0 - S_1 u_0 - S_2 u_0 (u_0^2 + w_0^2) \quad (27)$$

Where S_4 is the frequency of the slow flow limit cycle oscillation corresponding to the frequency of the QP modulation. The solution up to the first-order is written as

$$u_0(T_0, T_1) = R(T_1)\cos(S_4 T_0 + \psi(T_1)) - \alpha_2 \quad (28)$$

$$w_0(T_0, T_1) = -R\sin(S_4 T_0 + \psi(T_1)) \quad (29)$$

Where R and ψ are, respectively, the amplitude and the phase of the QP modulation and $\alpha_2 = \frac{S_3}{S_4}$. Substituting (28) and (29) into (21) and removing secular terms gives the following autonomous slow-modulation equations

$$\begin{cases} \frac{dR}{dt} = (S_1 + 2S_2\alpha_2^2)R + S_2R^3 \\ R\frac{d\psi}{dt} = 0 \end{cases} \quad (30)$$

Equilibria of this slow-modulation system determine the QP solutions of the original equations (3), (4). The nontrivial equilibrium obtained by setting $\frac{dR}{dt} = 0$ is given by

$$R = \sqrt{-\frac{S_1+2S_2\alpha_2^2}{S_2}} \quad (31)$$

Consequently, the approximate periodic solution of the slow flow (21) is given by

$$u(t) = R\cos(\theta t) - \alpha_2 \quad (32)$$

$$w(t) = -R\sin(\theta t) \quad (33)$$

The approximate amplitude $a(t)$ of the QP response reads

$$a(t) = \sqrt{R^2 + \alpha_2^2 - 2\alpha_2 R\cos(\theta t)} \quad (34)$$

and the envelope of the QP modulation is delimited by a_{min} and a_{max} given by

$$a_{min} = \min\{\sqrt{R^2 + \alpha_2^2 \pm 2\alpha_2 R}\} \quad (35)$$

$$a_{max} = \max\{\sqrt{R^2 + \alpha_2^2 \pm 2\alpha_2 R}\} \quad (36)$$

and the explicit expression of the QP response of the original equation (3) is written as

$$x(t) = u(t)\cos(\omega t) + w(t)\sin(\omega t) \quad (37)$$

On the other hand, the QP solution of the voltage $v(t)$, obtained by inserting Eq. (37) into Eq. (2), can be extracted via a convolution integral with the boundary condition $v(0) = v(T)$ where $T = \frac{2\pi}{\nu}$. This leads to

$$v(t) = -\kappa e^{(\lambda e^{\lambda\tau}-\mu)t}\int_0^t \dot{x}(t')e^{(\mu-\lambda e^{\lambda\tau})t'}dt' \quad (38)$$

Consequently, the power, the average and the maximum powers output in the QP regime are given, respectively, by

$$P_{QP}(t) = \lambda(-\kappa e^{(\lambda e^{\lambda\tau}-\mu)t}\int_0^t \dot{x}(t')e^{(\mu-\lambda e^{\lambda\tau})t'}dt')^2 \quad (39)$$

$$P_{avQP} = \frac{\mu\kappa^2\nu^2}{2[(\mu-\lambda\cos(\omega\tau))^2+(\nu+\lambda\sin(\omega\tau))^2]}a^2 \quad (40)$$

$$P_{maxQP} = \frac{\mu\kappa^2\nu^2}{[(\mu-\lambda\cos(\omega\tau))^2+(\nu+\lambda\sin(\omega\tau))^2]}a^2 \quad (41)$$

Where $\nu = S_4$ is the frequency of the QP modulation and a in Eqs. (40), (41) is now derived from Eqs. (35), (36).

Figure 2 shows the variation of the amplitudes a of the periodic and the QP responses as well as the corresponding output power amplitudes (P_{max}, P_{maxQP}) versus the frequency ω in the case of the undelayed circuit of the harvester ($\tau = 0$). The periodic response is given by (17) and the boundaries of the QP modulation envelope are obtained from Eqs. (35), (36). Also, the maximum powers for periodic and QP vibrations are given, respectively, by Eqs. (20),and (41). For validation, the analytical prediction (solid lines for stable and dashed line for unstable) are compared to numerical simulation (circles) obtained by the method of Runge Kutta of order 4. The plots in Fig. 2b show that in the absence of time delay, the performance of the QP vibration-based energy harvesting is better than that of the periodic vibration.

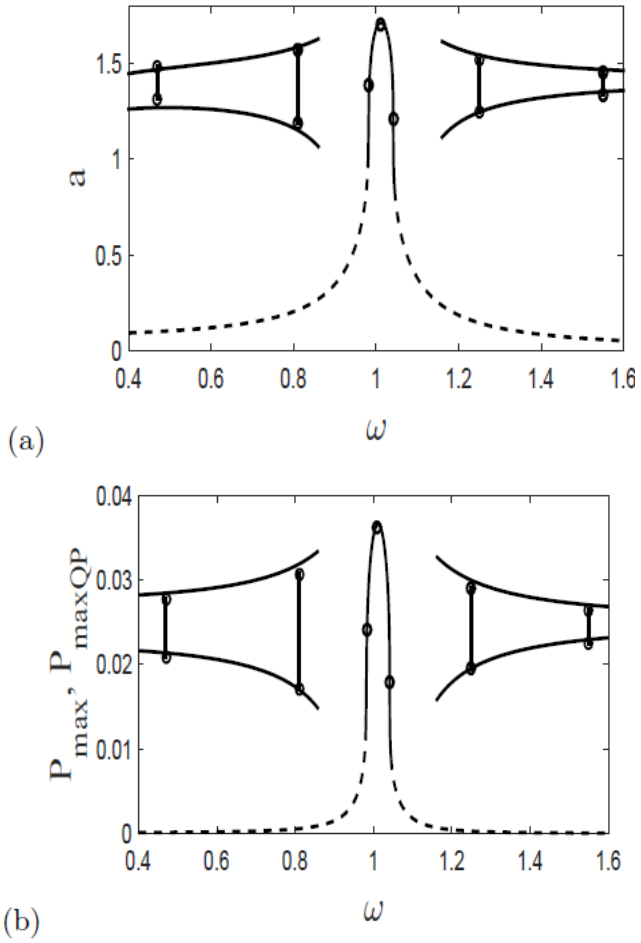

Figure 2: Vibration and power amplitudes vs ω for $\alpha = 0.1$, $\beta = 0.2$, $\chi = 0.05$, $\lambda = 0.05$, $\kappa = 0.5$, $f = 0.08$ and $\tau = 0$. Analytical prediction (solid lines for stable and dashed line for unstable) and numerical simulation (circles).

In Fig. 3 is shown the influence of time delay introduced in electrical component on the EH performance of the system. The curves given by the red lines correspond to this case of delayed harvester ($\tau = 6.2$). For comparison, we plot also in black the case where the delay is absent ($\tau = 0$). The analytical prediction (solid lines for stable and dashed line for unstable) are compared to numerical simulation indicated by circles obtained by using dde23 algorithm [11]. Here, it can be observed that introducing the delay in the electrical circuit causes a significant increase of the output power over a certain range of the frequency ω.

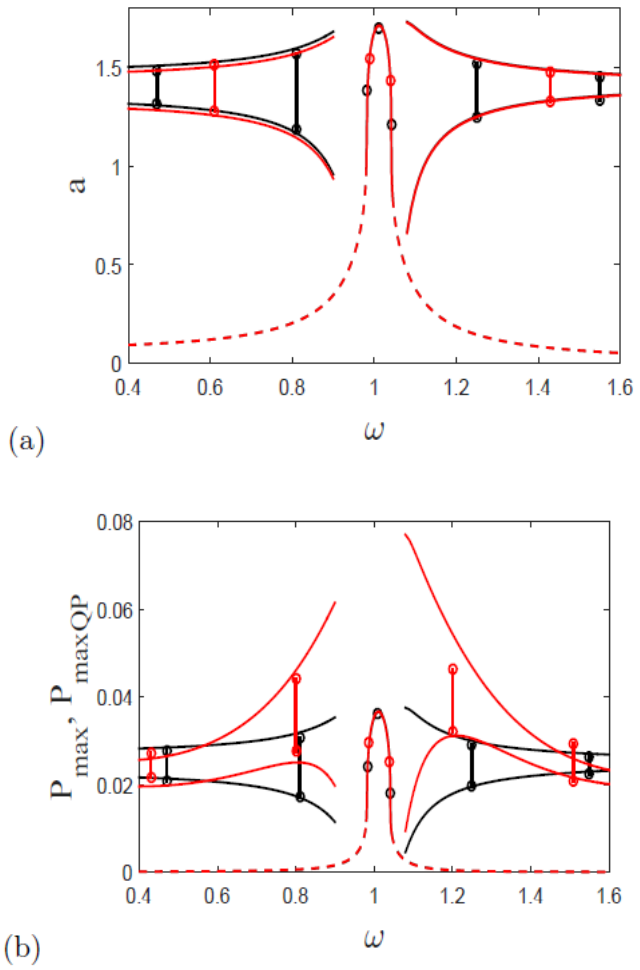

Figure 3: Vibration and power amplitudes vs ω for $\alpha = 0.1$, $\beta = 0.2$, $\chi = 0.05$, $\lambda = 0.05$, $\kappa = 0.5$ and $f = 0.08$. Analytical prediction (solid lines for stable and dashed line for unstable) and numerical simulation (circles). Red lines for delayed electric circuit ($\tau = 6.2$) and black lines for undelayed circuit ($\tau = 0$, Fig. 2).

To guarantee the robustness of the QP vibration during energy extraction operation, it is important to perform the stability analysis of the QP solution and obtained the stability chart of the nontrivial solution of the slow-slow flow (30). This can be obtained by calculating the eigenvalues of the

Jacobian matrix J of the slow-slow flow (30). The curves delimiting the regions of existence of the QP oscillations and the domains of their stability are given by the conditions ($\mathrm{Tr(J)} = -2S_1 - 4S_2\alpha_2^2 < 0$ and $\mathrm{Det(J)} = 0$).

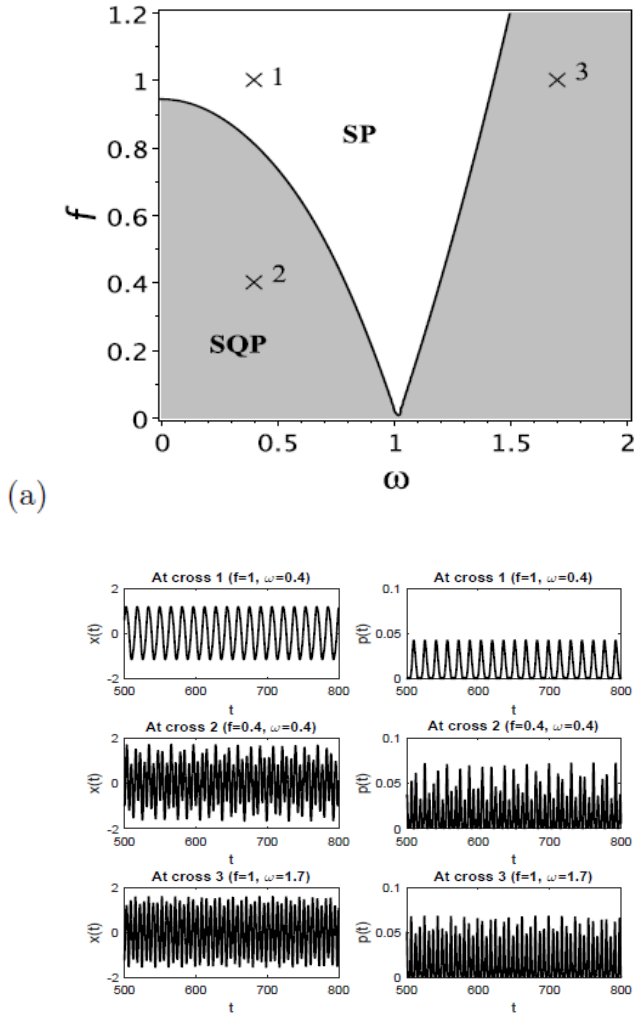

Figure 4: (a) Stability chart in the plane (f, ω), (b) time and power histories corresponding to different regions picked from (a). SP: stable periodic, SQP: stable QP; $\alpha = 0.1$, $\beta = 0.2$, $\chi = 0.05$, $\lambda = 0.05$, $\alpha = 0.1$, $\kappa = 0.5$, and $\tau = 6.2$.

Figure 4a shows this stability chart of the QP solution in the parameter plane (f, ω) for $\tau = 6.2$ indicating the (grey) regions where stable QP (SQP) solutions take place and the (white) region corresponding to stable periodic (SP) solutions. In Fig. 4b are shown time histories and the corresponding power output responses related to crosses labelled 1, 2, 3 in Fig. 4a. From cross 1 to cross 2 or 3 the system response bifurcates from SP to SQP oscillations via secondary Hopf bifurcation producing, as expected, a slight modulation of the amplitude response and a significant performance of the power output. At the bifurcation, the SP response turns into unstable.

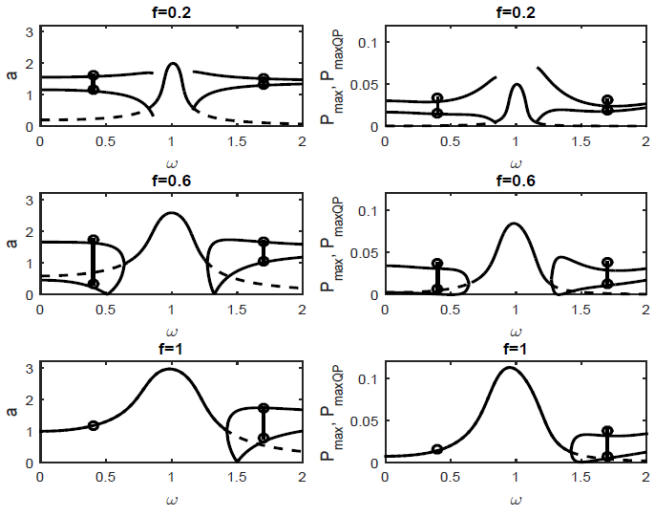

Figure 5: Vibration and powers amplitudes vs ω at different values of $f = 0.2, 0.6, 1$; for $\alpha = 0.1$, $\beta = 0.2$, $\chi = 0.05$, $\lambda = 0.05$, $\kappa = 0.5$ and $\tau = 6.2$. Analytical prediction (solid lines for stable and dashed line for unstable) and numerical simulation (circles).

Figure 5 depicts analytical results of the amplitude response and the maximum powers (P_{max}, P_{maxQP}) as function of ω for $f = 0.2, 0.6, 1$. The analytical predictions of the periodic response and the QP modulation envelope (solid lines) are compared to results obtained by numerical simulations (circles) for validation. for low value of the amplitude of the harmonic excitation $f = 0.2$, the QP solutions

is more than the periodic one, for increasing the f for $f = 0.6$ or $f = 1$ the periodic solutions in this case become more important with hight amplitude comparing with the QP solutions.

IV. Conclusions

In conclusion, we have studied the EH performance in a van der Pol forced oscillator coupled to a delayed piezoelectric harvester device. The analysis is carried out near the primary resonance and a perturbation techniques are performed to obtain approximation of periodic and QP vibrations which are exploited to harvest energy. We have explore the influence of time delay in the piezoelectric subsystem on the EH performance of the harvester. Specifically, it was shown that in the presence of time delay in the electrical circuit there exist an optimum value of the frequency for which the QP vibrations amplitude and the output power are maximum. To guarantee the robustness of the QP vibration during energy extraction operation a stability analysis was performed and the QP stability chart was determined.

Appendix

$$S_1 = \frac{\alpha}{2} - \frac{\kappa\chi(\mu - \lambda\cos(\omega\tau))}{2(\mu - \lambda\cos(\omega\tau))^2 + 2(\omega + \lambda\sin(\omega\tau))^2}$$

$$S_2 = \frac{-\beta}{8}, \quad S_3 = -\frac{f}{2\omega}$$

$$S_4 = \frac{\sigma}{2\omega} + \frac{\kappa\chi(\omega + \lambda\sin(\omega\tau))}{2(\mu - \lambda\cos(\omega\tau))^2 + 2(\omega + \lambda\sin(\omega\tau))^2}$$

References

[1] Z. Ghouli, M. Hamdi, F. Lakrad, M. Belhaq, Quasiperiodic energy harvesting in a forced and delayed Duffing harvester device. Journal of Sound and Vibraton, 407, 271-285, (2017).

[2] Z. Ghouli, M. Hamdi, F. Lakrad, M. Belhaq, Energy harvesting in a delayed and excited Duffing harvester device. MATEC Web of Conferences, 83, 02001, (2016).

[3] Z. Ghouli, M. Hamdi, M. Belhaq, Improving energy harvesting in excited Duffing harvester device using a delayed piezoelectric coupling. MATEC Web of Conferences, 241, 01010, (2018).

[4] M. Belhaq, M. Hamdi, Energy harversting from quasi-periodic vibrations. Nonlinear Dynamics, 86, 2193-2205, (2016).

[5] Z. Ghouli, M. Hamdi, M. Belhaq, Energy harvesting from quasi-periodic vibrations using electromagnetic coupling with delay. Nonlinear Dyn, 89, 1625-1636, (2017).

[6] M. Belhaq, Z. Ghouli, M. Hamdi, Energy harvesting in a Mathieu-van der Pol-Duffing MEMS device using time delay. Nonlinear Dyn, 94, 2537-2546, (2018).

[7] Z. Ghouli, M. Hamdi, M. Belhaq, The Delayed van der Pol Oscillator and Energy Harvesting. M. Belhaq (eds) Topics in Nonlinear Mechanics and Physics. Springer Proceedings in Physics, 228, Springer, Singapore, (2019).

[8] Z. Ghouli, M. Hamdi, M. Belhaq, Energy Harvesting in a Duffing Oscillator with Modulated Delay Amplitude. I. Kovacic, S. Lenci (eds) IUTAM Symposium on Exploiting Nonlinear Dynamics for Engineering Systems. ENOLIDES 2018. IUTAM Bookseries, 37, Springer, Cham, (2020).

[9] A.H. Nayfeh, D.T. Mook, Nonlinear Oscillations, Wiley, New York, (1979).

[10] M. Belhaq, M. Houssni, Quasi-periodic oscillations, chaos and suppression of chaos in a nonlinear oscillator driven by parametric and external excitations. Nonlinear Dyn. 18, 1-24, (1999).

[11] L.F. Shampine, S. Thompson, Solving delay differential equations with dde23, PDF available on-line at http: //www.radford.edu/~ thompson/webddes/tutorial.pdf, (2000).